Effects of Sea Bed Structure on High Frequency Acoustic Reverberation in Shallow Water

Heidi A. Terrill-Stolper, Roger W. Meredith

Naval Research Laboratory
Bldg. 1005, Code 7174
Stennis Space Center, MS 39529
Email: terrill@zoe.nrlssc.navy.mil, meredith@vixen.nrlssc.navy.mil

and

Melvin D. Wagstaff

Planning Systems, Inc.
115 Christian Lane
Slidell, LA 70458
Email: mel_wagstaff@psislidell.com

Abstract

Although undoubtedly sea bed structures, patterns, and composition affect the reverberation of high-frequency acoustic energy, the extent of their influence is not well known. The effects of varying selected bedform parameters for sandy sea floors in shallow water at two depths are modeled. Visible changes are observed for different bedform patterns and sandwavelength changes of ~0.5 m. Changes of 0.05 in the sand wave height-to-length ratio are statistically detectable.

1. Introduction

One of the challenges in sonar operation is identifying the signature of a real "target" in the clutter produced by the environment. The sea floor, including material, structure and pattern, is one source of environmental clutter. Furthermore, in addition to background interference, variability of the sea floor structure and parameters can produce constructive interference, or "false" targets, that mimic real targets.

The purpose of this research is to help characterize the effects of bathymetry on general sonar operations and, specifically, in mine hunting tasks. This includes investigating the types of sea bed parameters that lead to the production of false targets, assessing the role of bathymetry in target fading of mine hunting sonars, and determining if range dependent bathymetry is relevant to mine hunting sonars. A full understanding also requires a general assessment of how bathymetry affects the statistical variability of bottom reverberation.

2. Method

2.1. Bathymetry Model

Observations have shown that sand covered regions of the sea floor are relatively dynamic with wave- or current-generated bedforms occurring from depths of a few centimeters near a beach to as much as 200 m on the continental shelf [1]. Wave generated sand waves are generally symmetric, having patterns classified as long-, intermediate-, and short-crested, brick, and random. Current or wave-current generated sand wave patterns include long crested, wavy (sinuous), cuspate, linguoid, as well as asymmetric versions of the wave generated sand waves.

The bathymetry-generation model developed for this study allows for choice of symmetric or asymmetric sand waves, maximum sand wave height, h, and length, λ, sand wave pattern (currently, choices are long-crested, short-crested, and random), and orientation of the sand wave pattern with respect to the primary observation direction. Although it is possible to combine several overlying sand bedforms (i.e., sand ripples formed on larger sand waves or dunes, and/or a sloping bed), these features have not been implemented in the present study.

The sand wave height equations used to generate the symmetric (wave-generated) and asymmetric (primarily current-generated) bedforms are modified from the equation given in Sleath [2] for symmetric sand ripples. For symmetric sand waves, the equation was modified to have the sand wave height run from zero to a maximum desired sand wave height, and the equation for ξ was abbreviated to first order. In the symmetric sand wave case the equation for sand wave height, y, is

$$y = \frac{h}{2}(1 + \cos k\xi) \tag{1}$$

$$\xi \equiv x + \frac{h}{2}\sin kx \tag{2}$$

where h is the maximum sand wave height, k is the wave number, and x is the range along the beam path.

In the asymmetric case, the equation was modified by the addition of a phase angle, ϕ; all other parameters are unchanged. The value of ϕ determines the extent of the asymmetry. Calibration of the phase factor to the symmetry parameter is not yet complete, therefore no determination as to the affect of the symmetry parameter on the reverberation has been attempted. Furthermore, some of the sand waves that have been classified as asymmetric may be either essentially symmetric or unrealistic since selection of the phase factor in the present study was random. The asymmetric sand wave equation is

$$y = \frac{h}{2}(1 + \cos[k\xi + \phi]). \tag{3}$$

Each bathymetry generated has a built-in random factor. For the long-crested sand waves, this is a randomly selected phase shift. In the symmetric case, the phase shift is implicitly included in value of x, altering the starting point on but not the shape of the sand wave profile. It is separated explicitly as the phase factor, ϕ, for the asymmetric case. Figure 1 (a.-b.) shows the effect of the phase shift on the shape of the sand wave profile. Figure 1a. is a 10 m wavelength, symmetric sand wave, as defined by (1), with a phase shift of 90°, or 2.5 m, implicitly included in the value of x. Figure 1b. shows the same sand wave with the phase shift now explicitly included as the factor ϕ in (3). Defining the direction of increasing range towards the shore, this sand wave has a symmetry parameter of .325, as defined by Inman [3].

Short-crested sand waves, defined by Inman [3] as sand waves having crest lengths between 1 and 3 λ, are all started in the trough, with the crest length and position along the crest determined randomly for each successive sand wave. If the randomly selected position on the sand wave is within 0.25λ of either end of the crest, then the sand wave amplitude, h, is linearly interpolated from between 0 and the selected wave height coordinated with the distance from the end of the crest. Figure 1c. demonstrates the effect of this random variation in sand wave amplitude along a single radial.

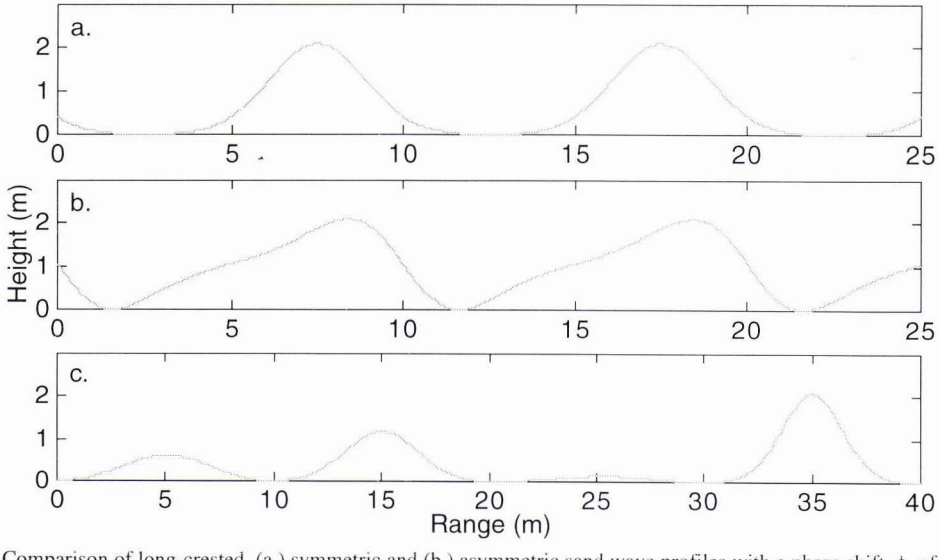

Figure 1: Comparison of long-crested, (a.) symmetric and (b.) asymmetric sand wave profiles with a phase shift, ϕ, of 90° and (c.) short-crested, symmetric sand wave profile. Sand wavelength is 10 m, height-to-length ratio is .21.

2.2. **The Reverberation Imaging Program (RIP)**

The Reverberation Imaging Program (RIP) [4] uses a modified ray trace model from the Naval Research Laboratory (NRL) range-dependent active system prediction (RASP) model [5]. Input for the model includes sound speed profiles for each beam path, sonar data, bathymetry files, and sea floor material, with choices ranging from mud to rock. Other environmental data, such as the surface, bottom, and volume loss and scatter may be user supplied or based on standardized models. The model calculates a one dimensional directional derivative along each beam pathway by linearly interpolating between

successive bathymetry points for use in determining the backscatter from a ray impact point. Model output consists of reverberation level versus time step.

2.3. **Modeled Sonar and Environment**

The sonar parameters including pulse length, frequency, and source level (dB re 1 microPa/Hz) are based on the SQQ-14 sonar. The sonar is placed at a depth of 20 m, with a 5° down tilt. The vertical profile is "standardized," with rays traced out to ±88 degrees from the sonar center with an interval of one ray every 1° for angles greater (less) than +21° (-21°), from +14° (-14°) to +21° (-21°) with an interval of one ray every 0.2°, and from +14° to -14° with an interval of one ray every 0.1°. The pulse length is 0.001 seconds, the center frequency is 80 kHz, and the source level is 224.0 dB re 1 microPa/Hz. Although the RIP program takes as input specific sonar parameters, the output is the reverberation off the sea floor, not the traditional sonar screen output.

The modeled environment consists of a typical shallow water summer sound speed profile (ssp), modified from a real summer ssp measured near Panama City, Florida. The ocean surface is assumed to be flat. Surface, bottom, and volume loss are based on standard models. The sea floor sand is taken to be medium grained sand over the total range for all beams. The same sound speed profile was used in RIP for each beam path. This ssp was measured at intervals of approximately 1 meter to a depth of 30 m. RIP runs are made at depths of 35 and 100 m. Consequently, the measured sound speed profile was modified by changing the depth of the last measured value to 100 m, making it appropriate for use at both the model depths. This modification is reasonable for the 35 m depth, since the water temperature, salinity, and pressure are unlikely to have changed significantly over 5 m. However, this is not necessarily the case for the 100 m depth. It is estimated, using the sound speed equation from Clay and Medwin [6], that between the actual measured depth of 30 m and the model depth of 100 m, there would be a change in the sound speed on the order of 5 m/s, assuming an average water temperature of about 15.6° C, and a temperature change on the order of 2° C, and constant salinity. Colder water would result in a greater difference in the sound speed, as would greater temperature changes. However the worst case sound speed change is estimated to be ~15 m/s, assuming a temperature change of 4° C (measured from Arctic data [7]) and water temperatures from 11.6° C to 15.6° C. Since the primary focus of this research is changes in the reverberation with bathymetry changes, this discrepancy in the sound speed at the maximum depth has been neglected, but further investigation of the influence ssp has on the reverberation is planned.

The pulse length determined the minimum sand wavelength allowed. The minimum allowed step size (in meters) was determined from the pulse length, T (in seconds), using the relation

$$(c/2) \times T \tag{4}$$

where c is the sound speed, taken in this case to be 1500 m/sec. For the SQQ-14 sonar, this translates to a 0.75 m minimum step size. The minimum sand wavelength allowed is then no less than 5 times the minimum step size. Each bathymetry file consists of 800 range/height pairs, calculated from the bathymetry model described above. The range of interest was 1000 m, with the actual step size used being the smaller of one fifth of the sand wavelength or 1.25156 m, the step size required to give 800 data points ranging from 0 to 1000 m.

This research concentrates on symmetric and asymmetric sand waves having long- and short-crested patterns. Sand wavelengths range from 7.5 m to 15 m, with height-to-length ratios from .05 to .21. The sand waves grow out of a flat bed at the selected depth; each depth choice (35 m and 100 m) is the maximum depth of the sea bed at that level. Figure 2 shows pseudocolor plots of the long- and short-crested sand wave bathymetries. The selected wavelength is 10 m, the height-to-length ratio (htlr) is .21.

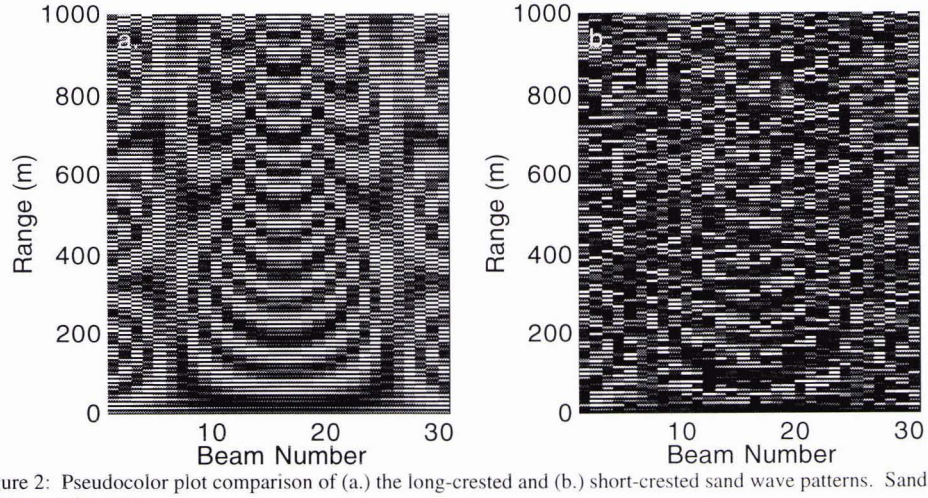

Figure 2: Pseudocolor plot comparison of (a.) the long-crested and (b.) short-crested sand wave patterns. Sand wavelength is 10 m., htlr = .21.

Thirty-one beams are used to construct the reverberation plots. These beams are numbered 1 to 31, with the center beam, beam number 16, defined as the primary observation direction. The horizontal beam width is 2°, so the 31 beams span an angular width of 60°, or ±30° on either side of the primary observation direction. RIP employs scattering angles measured in the vertical plane containing the sonar and the scattering point. No horizontal scattering component is currently included when computing reverberation. Evaluation of sea beds having orientations other than perpendicular to the primary observation direction is deferred until a horizontal component is included in the scattering. Beams 12 to 16 are used to obtain statistical results.

3. Results

The output of RIP was studied both directly through graphical examination of the model output and indirectly through a variety of statistical methods. Each of these methods has different strengths, and reveals different features of the simulated reverberation. The two depths have been treated separately, but comparisons between the results for other input parameters for a given depth have been made.

3.1. 100 meter depth

At the 100m depth, at least three RIP runs were completed for each of the selected symmetric case parameter sets, and one RIP run for each of the asymmetric parameter sets. The additional RIP runs completed for the symmetric case at this depth have greatly improved the reliability of the statistical results.

The reverberation at this depth has much more variability than that at the shallower depth. Reverberation returns start at about .1 seconds after the start of the time series. In the region between .1 and .4 seconds the reverberation has minimal variation, except for the presence of two "dark" bands. After about .4 sec, return from the main "beam" of the sonar starts. This region is characterized by relatively high variation in the reverberation. Although the magnitude of the variability of the reverberation reduces with time through this region, the average reverberation level does not change substantially. Eventually, the overall variation in the reverberation drops to negligible levels, but, unlike the reverberation for the 35 m depth which tends to smooth out completely, there are still "bright" spots or peaks in the reverberation all the way to the end of the time series, at about 1.3 sec. Figure 3 shows a comparison of the pseudocolor plots of the reverberation from the 10 m wavelength, htlr = .21 long- and short-crested bedforms at 100 m. The shading is scaled from darkest, reverberation level 30 dB, to lightest, reverberation level of 110 dB.

The reverberation histograms show a consistent pattern of narrowing the total reverberation range as the htlr is lowered. This shift in the shape of the reverberation histogram is most obvious in the short-crested symmetric sand wave case. Figure 4, shows the changes in the reverberation histograms with the height-to-length changes for the 100 m depth.

3.1.1. *Symmetric Sand Waves*

Symmetric sand waves were modeled in both the long- and short-crested wave patterns for wavelengths of 7.5, 8.0, 10.0, 12.5 and 15.0 m, and wave height-to-length ratios of .05, .10, .15, and .21.

A sand wavelength change of 0.5 m (7.5 m to 8.0 m) is detectable for the long-crested symmetric sand waves at this depth, but cannot be consistently identified for short-crested sand waves. Changes of 2 and 2.5 m, however, are readily detected for both sand wave types. Changes in the sand wavelength may be easier to detect for smaller height-to-length ratios, since the reverberation from the lower height to length ratios generally have fewer areas in the reverberation plot where the return from the sand wave is unusually high.

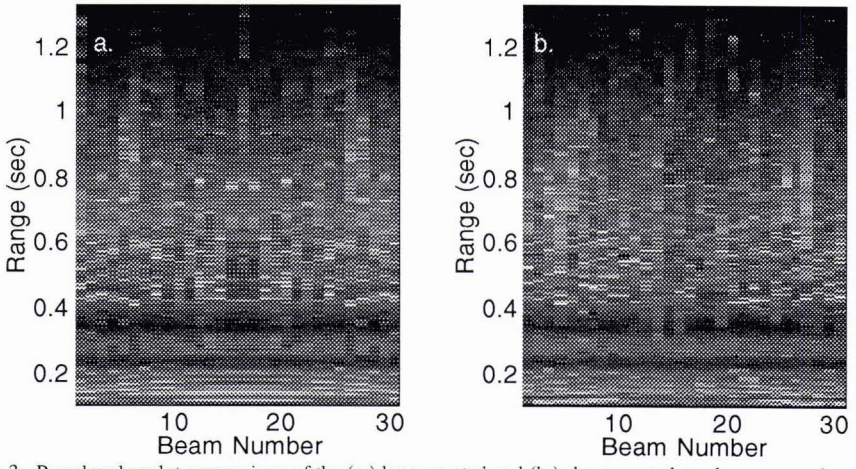

Figure 3: Pseudocolor plot comparison of the (a.) long-crested and (b.) short-crested sand wave reverberation at the 100 m depth. Sand wavelength is 10 m, htlr = .21.

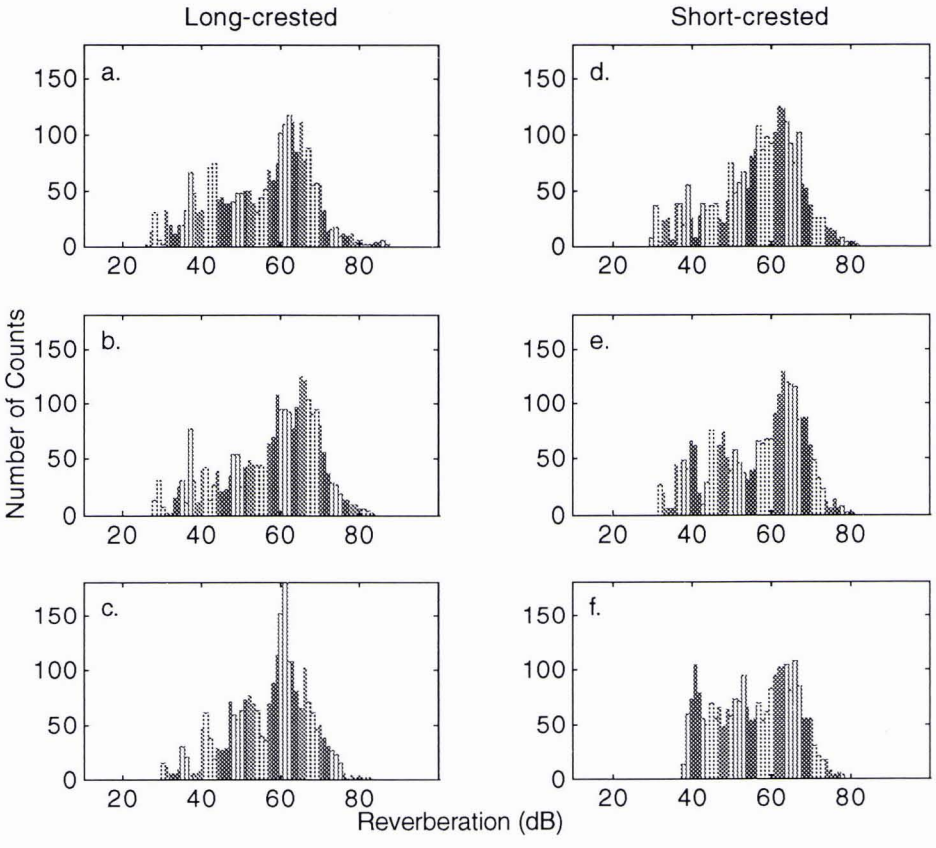

Figure 4: Comparison of the reverberation histograms of symmetric sand waves. For long-crested sand waves, a.) htlr = .21, b.) htlr = .15, c.) htlr = .10. and for short-crested sand waves, d.) htlr = .21, e.) htlr = .15, f.) htlr = .10.

Interestingly, although the reverberation histograms of the long- and short-crested sand waves show a similar pattern, the patterns of the mean reverberations are not consistent. The long-crested sand waves have the lowest mean reverberation for the htlr .05 at around 54 dB, the next lowest mean reverberation is at htlr .21, at about 55.5 dB, the highest mean reverberation is for htlr .15, averaging around 57.5 dB, with htlr .10 averaging about 57.0 dB. Short-crested sand waves with htlr .05 have the lowest mean reverberation, again around 54 dB, but the next lowest mean reverberation is for htlr .10, averaging around 56 dB, htlr .15 mean reverberation averages around 56.5 dB, and htlr .21 slightly higher.

Not only do short-crested sand waves have smaller variability in the centroid and mean reverberation levels between the various height-to-length ratios, but greater variability between the mean reverberation values for sand waves having the same parameters than do the long-crested sand waves. This is attributed to the variability in the maximum sand wave height when the beam path intersects the ends of a sand wave crest.

3.1.2. *Asymmetric Sand Waves*

Asymmetric sand waves were modeled in the long-crested wave pattern for wavelengths of 7.5 and 10.0 m, with wave height-to-length ratios of .10, .12, .15, .193, and .21, wavelength 7.75 m with height-to-length ratio .21, and wavelength 8.0 m, height-to-length ratios of .10, .15, and .21. Wavelengths 7.5, 8.0, 10.0, and 15.0 m with height-to-length ratios .10, .12, .15, .193, and .21 were modeled in the short-crested wave pattern.

Although the shape of the reverberation peaks and troughs in the long-crested case varies between the different sand wave parameter choices, the variation cannot be coordinated to the change in the shape of the sand wave with changes in starting phase. Modeled short-crested asymmetric sand waves had the same shape, since the starting phase was the same for all. Further study into the effect on the reverberation of the shape of the asymmetric sand wave is planned.

Differentiating between reverberation plots having sand wavelength differences of 2.0 m or more is easily done for both sand wave patterns. For the long-crested sand wave pattern, differentiating between the reverberation plots with sand

wavelength differences of 0.5 m (7.5 to 8.0 m) can be done consistently, but requires much more careful examination of the reverberation plots. It is not always possible to differentiate between the 7.5 m and 8.0 m sand wavelength reverberation plots in the short-crested sand wave case.

3.1.3. *Comparison of Symmetric and Asymmetric Sand Waves at 100 m*

No differences in the reverberation plots can be detected between symmetric and asymmetric sand waves of similar sand wavelengths. In general, the larger the height-to-length ratio, the wider the reverberation range and the greater the frequency of high reverberation levels. This pattern is in accord with the idea that the greater height-to-length ratios increase the back scatter by providing a larger component of the gradient perpendicular to the acoustic ray path over larger areas of the sand wave.

3.2. **35 meter depth**

At the 35 m depth, one RIP run was done for each set of parameters selected. Statistical evaluation gave very little useful information; often there were no clear differences between the results for different parameters. As yet it is not clear if this lack of differentiation in the reverberation statistics is due to the low grazing angle of the main beam acoustic rays, the large distance (≥15 m) between points of impact of successive rays, or, since this problem is most obvious in the asymmetric case, inconsistency in sand wave shape.

The reverberation for this depth reaches its peak values in a short (time scale) region of high variability. This is followed by a more moderate region, starting between .2 and .3 sec., where the reverberation output follows the design of the sand wave, with the average reverberation level steadily decreasing. The highest times (from around 1.0 to 1.33 sec.) correspond to reverberation from the region beyond the sand wave field. This reverberation zone is generally flat, with the total return continuing to decrease. Often the last few time steps are accompanied by a sharp drop in the reverberation level. Figure 5 shows a comparison of the pseudocolor plots of the reverberation from the symmetric 10 m wavelength, htlr = .21, long- and short-crested bedforms at 35 m. The shading is scaled from darkest, reverberation level 10 dB, to lightest, reverberation level of 155 dB.

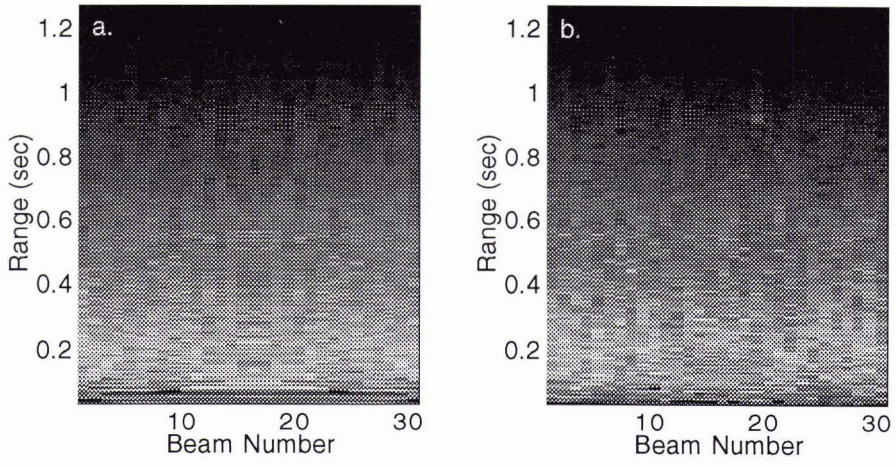

Figure 5: Pseudocolor plot comparison of the (a.) long-crested and (b.) short-crested symmetric sand wave reverberation at the 35 m depth. Sand wavelength is 10 m, htlr = .21.

3.2.1. *Symmetric Sand Waves*

Reverberation results were modeled for long-crested sand waves with the following parameters: wavelengths 7.5 m and 10.0 m, height-to-length ratios .10, .15, and .21; wavelength 8.0 m at height-to-length ratios of .05, .10, .15, and .21; wavelength 12.5 m, height-to-length ratios .05 and .10; and for wavelength 15.0 m, height-to-length ratios of .15 and .21. For short-crested sand waves, reverberation results were modeled for sea floors characterized by the following parameters: for wavelength 7.5 m; height-to-length ratios .10, .15, and .21, for wavelength 8.0 m, height-to-length ratio .05; for wavelength 10.0 m, height-to-length ratios .05, .10, .15, and .21; for wavelength 12.5 m, height-to-length ratio .15; and for wavelength 15.0 m, height-to-length ratios .10 and .21.

As with the sand waves at 100 m, differences in the sand wavelength were apparent in the reverberation. Long-crested sand waves having wavelengths of 7.5 m and 8.0 m could generally be differentiated. Variations in the sand wavelength of approximately 2 m were easily seen in both the short-crested and long-crested sand wave cases. A minimum change in the sand wavelength producing an observable change in the reverberation is currently under investigation. Changes in the height-to-length ratio were not obvious in the reverberation plots.

Although there is no clear differentiation between the reverberation histograms for most height-to-length ratios at the 35 m depth, in the symmetric, long-crested case, there is an indication of a trend towards a pattern that is consistent with the statistical results for long-crested sand waves at the 100 m depth in the mean values of the reverberation. This is continued in the centroids of the reverberation histograms of symmetric sand waves.

The most notable exception to the rule that reverberation plots for bathymetries are indistinguishable with respect to changes in height-to-length ratio (htlr) is htlr .05. Bathymetries having this htlr are easily identified in both the reverberation, and through statistical tools including the reverberation histograms, mean reverberation values, and the centroids of the reverberation histograms. They have significantly lower maximum levels of reverberation, and narrower total reverberation ranges, as seen in the reverberation histogram.

3.2.2. *Asymmetric Sand Waves*

Asymmetric sand waves were observed for long- and short crested sand waves having wavelengths of 7.5 m, 7.75 m, 8.0 m, and 10.0 m and height-to-length ratios of .10, .12, .15, .193, and .21. Asymmetric short-crested sand waves were also modeled at wavelength 15.0 m. A very limited number of "random" sand waves, consisting of 4-7 overlying, randomly oriented long-crested sand waves were also studied. These had sand wavelength ranges of 6.0--10.0 m, 7.5--12.5 m and 10.0--15.0 m, with sand wave heights based on a height-to-length ratio of .21 for the shortest wavelength of the selected range.

Direct observation of the reverberation showed that distinguishing between the different sand waves patterns is relatively easy, although the reverberation of the short-crested and long-crested sand waves have many features in common. Distinguishing between the different wavelengths and wave height-to-length ratios was not as straight forward. In a side by side comparison of the reverberation plots of the 7.5 m, 7.75 m, and 8.0 m sand waves, it was possible to distinguish between the 7.5 m wavelength and the 8.0 m wavelength, but the 7.75 m wavelength sand wave was not distinguishable from either of the other wavelengths. As the wavelength difference is increased, it becomes easier to distinguish between the reverberation results, with sand wavelength differences of 2 m easily detected. No significant, consistent differences were detected between the reverberation results with changes in the height-to-length ratio of the sand wave.

Statistical results were inconclusive for this data set. The reverberation histograms were essentially indistinguishable when comparing the various height-to-length ratios or the sand wave type. The centroids of the reverberation histograms, with the exception of the centroid of the short-crested sand waves for height-to-length ratio of .10 with a centroid reverberation level of 59 dB, were all confined within a range of approximately 0.5 dB located between 60 and 61 dB.

3.2.3. *Comparison of Symmetric and Asymmetric Sand Waves at 35 m*

There is very little noticeable difference between the reverberation plots for the symmetric and asymmetric sand waves at this depth. Furthermore, the reverberation histograms of the symmetric and asymmetric, and long- and short-crested sand waves are virtually indistinguishable for most height-to-length ratios (the exception is for height-to-length ratio .05, which has not been observed in the asymmetric case). However, other statistical methods reveal some differences. The means of the reverberation histograms of the asymmetric sand waves are randomly distributed, while those of the symmetric sand waves suggest a pattern, although there is not yet enough data to confirm this. The centroids of the reverberation histograms also support the suggestion of a trend in the mean for the symmetric case. Another difference is in the cumulative distribution functions (cdf) of the reverberation. Surprisingly, the symmetric sand waves show greater variation in cdf than do the asymmetric sand waves, even though the asymmetric sand waves have great variability in the sand wave shape, in addition to the random shifts previously discussed.

4. Discussion

The reverberation is generally consistent with the bathymetry producing it. The long crested sand waves, which were very symmetric, produces reverberation plots that show the symmetry of the bedform. Short crested sand waves that have a higher degree of randomness due to the variations in amplitude produce reverberation that demonstrates a higher degree of randomness than do the reverberation from long crested sand waves. However, reverberation plots often demonstrate substantial variability between nearby beam radials that is not seen in the bathymetry that produces them, and along a single radial they generally show less trough-to-peak variability. This is attributed to the effects of other environmental conditions to which the reverberation is subject.

Sand wavelength changes as small as 0.5 m could be detected in many circumstances, particularly for long-crested sand waves. Sand wavelength changes of 2 m could be detected for all sea bed patterns examined. Study to further narrow the threshold level for detectable wavelength change for each combination of sea bed parameters is in progress.

The reverberation from the 100 m depth is much more likely to have multiple occurrences of "false" targets, regions in the simulated reverberation where the return is much higher than the typical return of the beam path. This is true of all height-to-length ratios examined, except .05, which does not show a tendency towards "false" targets at 100 m. However, the overall peak reverberation levels and total reverberation range are lower at 100 m than at 35 m. Comparison of Figures 2, 3, and 5 gives an overview of the effects of bathymetry type and depth on the reverberation. Figure 2 shows a pseudocolor plot comparison of the long- and short-crested symmetric bathymetries and the corresponding reverberation plots are shown in Figure 5 for the 35 m depth and Figure 3 for the 100 m depth. The bedform parameters are sand wavelength, 10.0 m, and height-to-length ratio = .21. Although the plots shown are of the symmetric sand waves, there are no substantial differences in the results for the asymmetric sand waves.

5. Conclusion

It is clear that the sea bed structure can have a significant impact on high frequency acoustic reverberation in shallow water. As yet it is not possible to quantify the effects of the sea bed parameters, however, qualitative conclusions can be drawn. Although it was expected that higher sand wave height-to-length ratios would result in increased incidence of high reverberation levels, the effect is not obvious in the pseudocolor reverberation plots. It was not until the statistical results were examined that it became clear that as the sand wave height-to-length ratio is reduced, the number of high reverberation regions is reduced and the overall consistency of the reverberation is increased. Various sand wave types produce different reverberation patterns consistent with the bathymetry. Smaller changes in sand wavelength are evident for the more symmetric sea bed patterns.

6. Acknowledgments

This work was funded by the Office of Naval Research, with technical management by Naval Research Laboratory, Code 7170.

References

[1] D. A. Cacchione and D. E. Drake, "Shelf Sediment Transport: An Overview with Applications to the Northern California Continental Shelf," in *The Sea: Ocean Engineering Science*, New York, Wiley, ch. 21, pp. 729-773, 1990.

[2] J. F. A. Sleath, Sea Bed Mechanics. New York, Wiley, ch. 2, p. 70, 1984.

[3] D. L. Inman, "Wave-Generated Ripples in Nearshore Sands", Department of the Army Corps of Engineers, Technical Memorandum #100, Oct. 1957.

[4] M. D. Wagstaff, unpublished.

[5] L. B. Palmer and D. M. Fromm, "The Range-Dependent Active System Performance Prediction Model (RASP)," Naval Research Laboratory Technical Report # NRL/FR/5160-92-9383, 1992.

[6] C. S. Clay and H. Medwin, Acoustical Oceanography: Principles and Applications. New York, Wiley, ch. 1, p. 3, 1977.

[7] M. A. Wilson, "Volume Reverberation in the Fram Strait Marginal Ice Zone: May 1988," Naval Research Laboratory, Technical Report # NRL/FR/7174-93-9420, 1993.